

<Original>

A Study on the Extrusion of Anisotropic Materials with the Method of Moire Fringe Analysis

Hoon Huh*, Dong-Won Kim**

(Received Nov. 17, 1977)

모아레법에 의한 異方性材料의 押出에 관한 研究

허 훈·김 동 원

요 약

Johnson의 直交異方性材料押出時의 slip line 解를 모아레法으로 검토하였다. 모아레試片上에 slip line 場과 類似한 모아레무늬를 얻어 理論解와 비교하였으며, 모아레무늬 解析法으로 變形域의 相當 스트레인速度分布를 구하였다.

I. INTRODUCTION

The theory of plane strain for anisotropic materials was established by Hill¹⁾ in 1950, and its application was executed with the indentation by a flat rigid die. Thence, its application had been left untouched since it is so difficult to be adapted, while in sheet metal forming the theory of anisotropy has been often used.

The slip line field solution for the extrusion of an anisotropic material was obtained by Johnson and his coworkers²⁾ in 1973, who accomplished the application of the theory of anisotropy to the indentation of the material with finite depth^{3, 4)}.

On the other hand, the use of moire fringes for strain measurement has been studied widely in the past two decade and the moire equations have been developed for arbitrary master and specimen grid pitches and orientations; and for ease of measurement the master grating pitch and orientation may be changed at will during an experiment, and as a result the methods of moire analysis become powerful in the field of plastic deformation.

The method of moire analysis was improved and applied to the extrusion of isotropic materials by Kato and his coworkers⁵⁾ in 1968, and they obtained the analogous feature to the slip line field.

In this paper, the slip line field obtained by Johnson is compared and examined with the moire fringe analysis improved by Kato. And the distributions of the equivalent strain rates in deforming region are obtained from the method of moire analysis.

This paper is concerned with the case of the plane strain extrusion of anisotropic materials through frictionless wedge-shaped

*Graduate Student, Seoul National University

**Member, Seoul National University

Discussions on this paper should be addressed to the Editorial Department, KSME, and will be accepted until February 15, 1978.

II. MOIRE FRINGE ANALYSIS

Moire fringes result from the superposition of two or more geometric patterns consisting of fairly orderly and relatively closely spaced systems of curves, dots or other elementary figures. The loci of points of intersections of the superimposed patterns form light moire fringes. If one or more of the initial patterns are distorted, the moire fringes generally will change, thus providing the basis for the moire method of strain measurement.

Two families of moire fringes are obtained by the superposition of the master grating and specimen grating which both are composed of the two families of parallel straight-lines. When the master grating is rotated properly, it is found that two families of moire fringes become parallel to each other at the arbitrary concerning points.

There exist two rotating angles of the above state and the orientations of the parallel fringes are the directions in which there is no elongation and of maximum shear strain rate. That is, between the magnitudes of the principal strains and the rotating angles of master grating, some simple relations can be evaluated. Such a method of moire fringe analysis was suggested and evaluated by Kato⁹⁾.

The condition that two families of moire fringes become parallel to each other is

$$|b_{ij}| \{ (b_{11}-1)(b_{22}-1) - b_{12}b_{21} \} = 0 \quad (1)$$

where $[b_{ij}]$ is the transformation matrix of master grating position to specimen grating position.

For small deformation, the transformation matrix

$$[b_{ij}] = \begin{bmatrix} 1 + \epsilon_x & \gamma_{xy} - \omega \\ \gamma_{xy} + \omega & 1 + \epsilon_y \end{bmatrix} \quad (2)$$

where ϵ_x , ϵ_y and γ_{xy} are components of st-

rains and ω is the rotating angle. And the relation between the rotating angles and the magnitudes of the principal strains are

$$\begin{aligned} \epsilon_1 &= -\omega^N \cot \beta^N \\ \epsilon_2 &= \omega^N \tan \beta^N \end{aligned} \quad (3)$$

where $\omega^I = -\omega^{II}$, $\beta^I = -\beta^{II}$, $N=I, II$ and β is the anticlockwise orientation of the parallel fringes to the y -axis.

For finite deformation, the transformation matrix can be written as follows:

$$[b_{ij}] = \begin{bmatrix} C_{11} & C_{12} \\ C_{21} & C_{22} \end{bmatrix} \begin{bmatrix} \cos \bar{\omega} & -\sin \bar{\omega} \\ \sin \bar{\omega} & \cos \bar{\omega} \end{bmatrix} \quad (4)$$

where $[C_{ij}]$ is the matrix of the strain components only, that is

$$[C_{ij}] = \begin{bmatrix} \frac{1}{\gamma_{xy}} + \frac{\epsilon_x}{1 + \epsilon_y} & \bar{\gamma}_{xy} \\ \bar{\gamma}_{xy} & 1 + \epsilon_y \end{bmatrix} \quad (5)$$

Then, the relations between the rotating angles and the magnitudes of the principal strains are

$$\begin{aligned} \bar{\epsilon}_1 &= -\bar{\omega}^N \cot \beta^N + \bar{\omega}^{N^2} \left(\frac{1}{2} + \cot \beta^N \right) + 0(\epsilon^3) \\ \bar{\epsilon}_2 &= \bar{\omega}^N \tan \beta^N + \bar{\omega}^{N^2} \left(\frac{1}{2} + \tan \beta^N \right) + 0(\epsilon^3) \end{aligned} \quad (6)$$

$N=I, II$

When the deformation is in the condition of plane strain, from the condition of incompressibility, it can be found that

$$\bar{\omega}^N = \frac{\sin 4 \beta^N}{3 + \cos 4 \beta^N} \quad (7)$$

III. EXPERIMENT

III. 1. Experimental Procedures

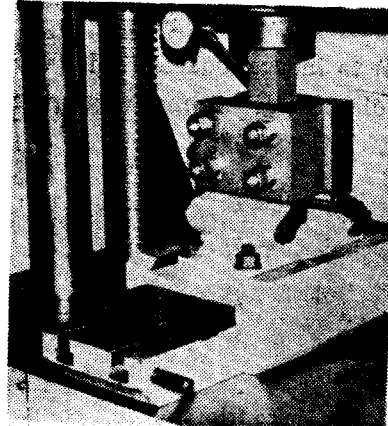


Fig. 1. Experimental extrusion apparatus

Table 1. The experimental condition of each specimens (Specimen dimension; 40×20 mm in section)

Specimen No.	Semi-angle of die	Fractional reduction	Orientation
1	15°	0.15	0° to compression direction
2	"	"	10° "
3	"	"	20° "
4	"	"	90° "
5	"	"	80° "
6	"	"	70° "
7	30°	0.2	0° "
8	"	"	10° "
9	"	"	20° "
10	15°	0.15	0° to rolling direction
11	"	"	10° "
12	"	"	20° "

Experiments were carried out with the experimental extrusion apparatus placed on the 30-ton universal testing machine, which is shown in Fig. 1.

Commercially pure aluminum ingot (99.5%) was cut out and annealed at 345°C for hours in salt bath. Then, to improve the anisotropic nature of the materials, some of the cut specimens were compressed with 40% reduction and others were rolled with 50% reduction, which are the well-known methods to induce considerable variations in the directional strength properties of

materials. Finally, the specimens were made with various orientations to the direction of compression and rolling and with two sorts of semi-angles of dies, which possess the different fractional reductions. They are listed in Table 1.

The parameters, T , which is a measure of the average resistance to deformation, and c , which specifies the state of anisotropy in the planes of flow, can be experimentally determined by two measurements, for example in compression tests, under condition of plane strain, at 0° and 45° to the axis of anisotropy with the governing equation¹⁾

$$\sigma = 2T \left(\frac{1-c}{1-c \sin^2 2\theta} \right)^{\frac{1}{2}} \quad (8)$$

To obtain moire fringes, the insides of split specimens were printed with the square grating whose pitch is 0.1 mm (250 lines/in.). The coating solution and dyeing stuff are T.P.R. which are of oil soluble type.

To secure the steady state flow, the specimens were extruded by 10 mm before the experiment and to obtain the strain rate in plastic region, they were extruded by 1mm after yielding. Extrusion was executed with the extrusion speed of 1.2 mm/min. And as a lubricant, motor oil H.D. 50 was used. For measuring the displacement, the dial gage whose scale is 0.01 mm was attached to the extrusion apparatus.

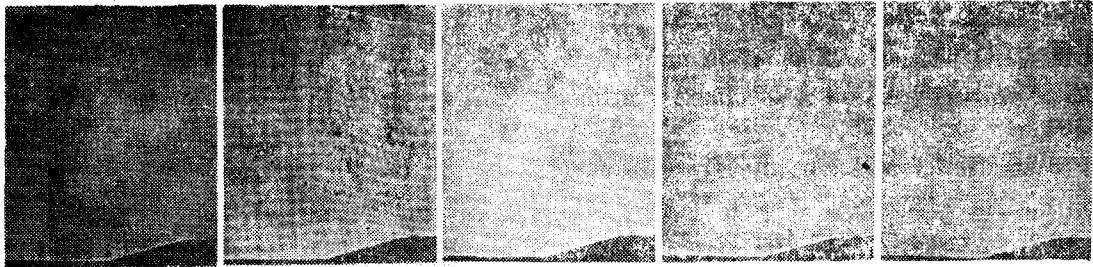


Fig. 2. Moire fringes which are parallel to each other with variation of rotating angles. Rotating angles; 6°, 3°, 0°, 3°, 6° respectively (Specimen No. 6)

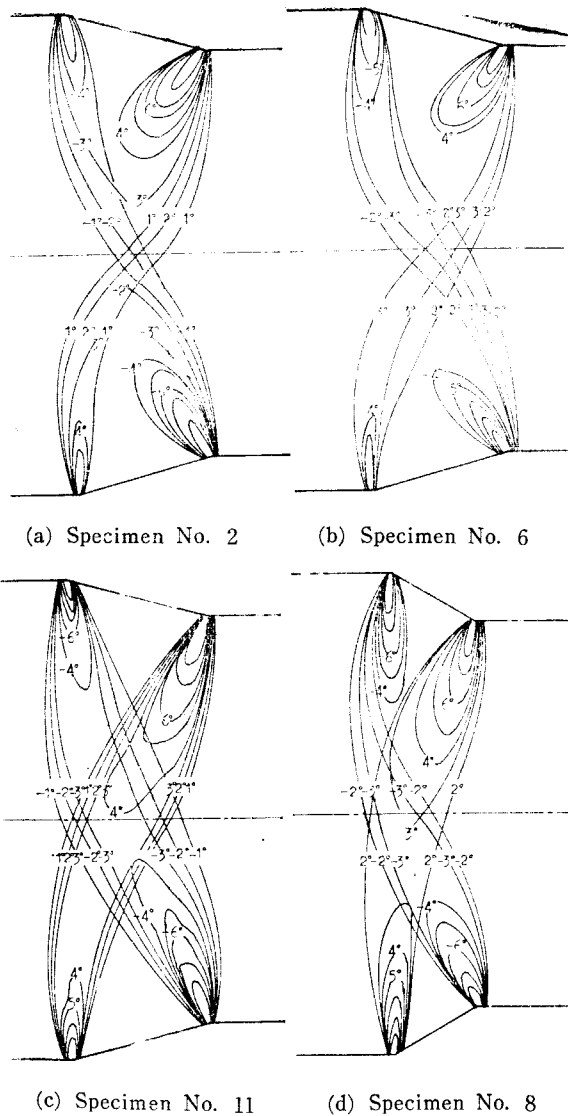


Fig. 3. Distributions of rotating angles

III. 2. Method of Analysis of Moire Fringes

The moire fringes which result from the superposition of the master grating and the deformed specimen grating are photographed with variations of the rotating angles of master grating from -10° to 10° at interval of 1° .

Before the analysis, rotating the master grating, the movement of the moire fringes

parallel to each other may be observed. Then, the growth and the position of the fringes in the neighborhood of the singular point can be distinguished and traced with ease. Examples of each moire fringes are shown in Figure 2, and the trajectories of the points where two moire fringes are parallel to each other are obtained as shown in Figure 3.

And the analogous feature of the slip line field can be obtained from the distribution of the rotating angles, as tracing the tangents of the trajectories.

The magnitudes indicated along the contour of Figure 6 are the values of the equivalent strain rates

$$\Delta\epsilon_{eq} = (2/\sqrt{3})\Delta\epsilon_1 \quad (9)$$

IV. RESULTS AND DISCUSSION

For the theory of plastic deformation, it is very important to predict and find the region of plastic deformation and to evaluate the strain rates in that region, which can be well examined by experiments and are sufficiently demonstrated by the moire fringe analysis in this paper.

The moire fringes analogous to the slip line fields are shown in Figure 4. The region of plastic deformation is divided into three parts, i.e., the part which is triangle-shaped and close to the die surface and has no fringe, the second part which is the neighborhood of singular points and has radiate fringes and the third part which is the middle of the plastic region and has cross fringes. If the movement of two families of moire fringes is observed, rotating the master grating and paying attention to the second part, it is found that the radiate fringes are composed of the folded ones of two families of moire fringes

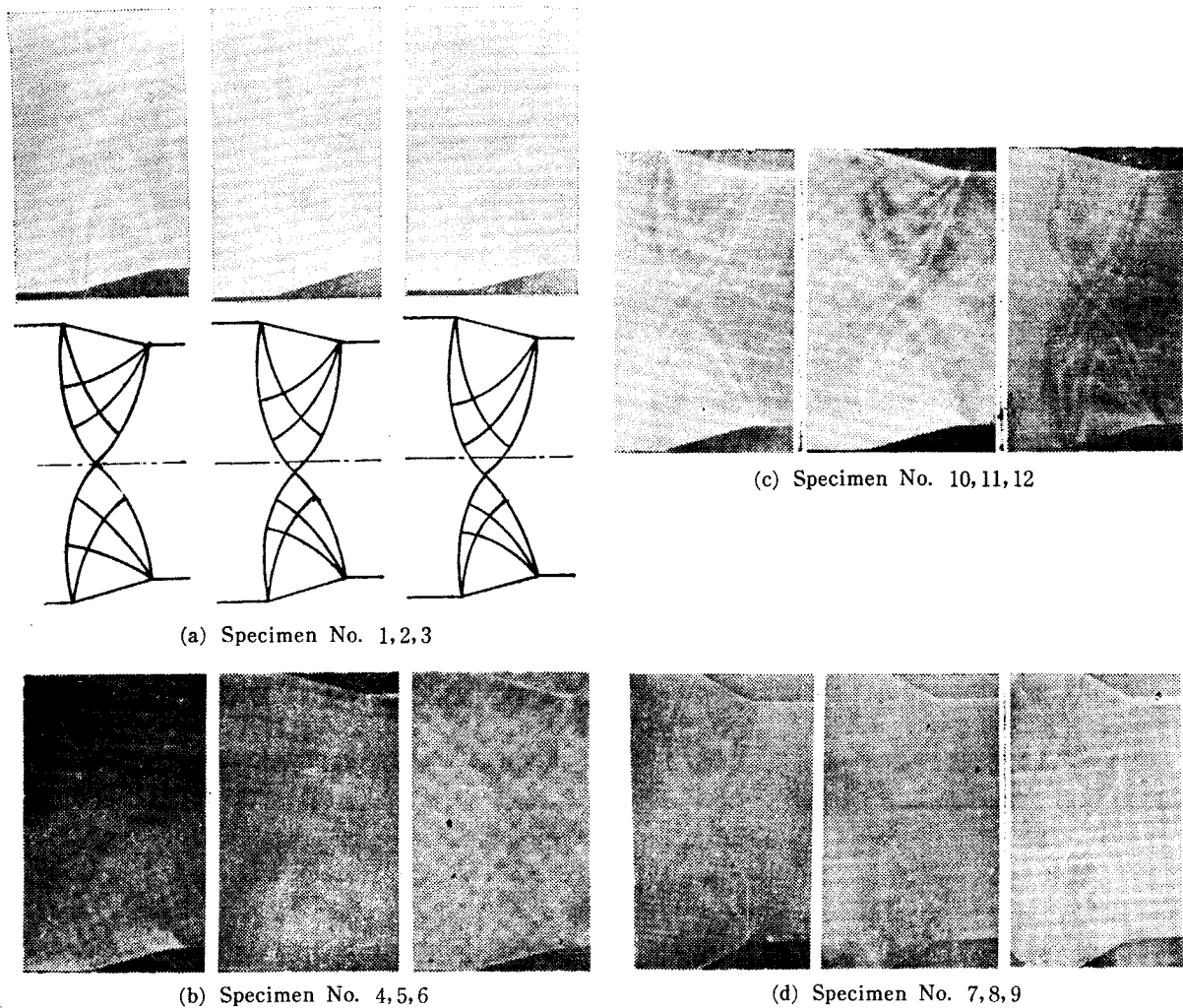


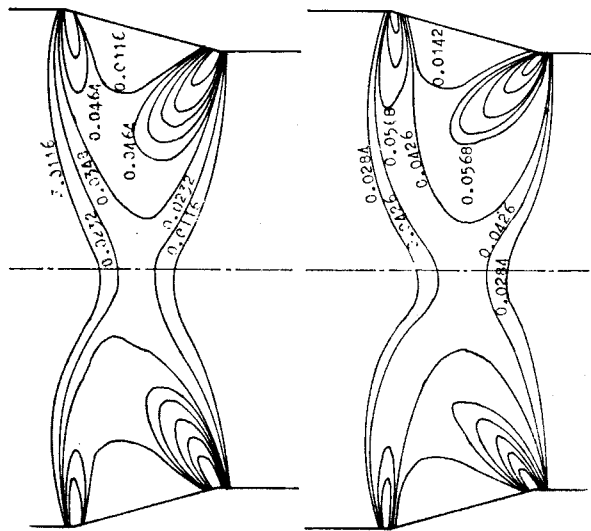
Fig. 4. The moire fringe analogous to slip line field

nges. So the radiate fringes mean the radiate lines of slip line field. And the distribution of the equivalent strain rates can be presumed from the density of moire fringes, which is high in the second part and is rare in the first part and become lower toward the center in the third part. So it is evident that the moire fringes are well coincident with the theoretical solution of the slip line field.

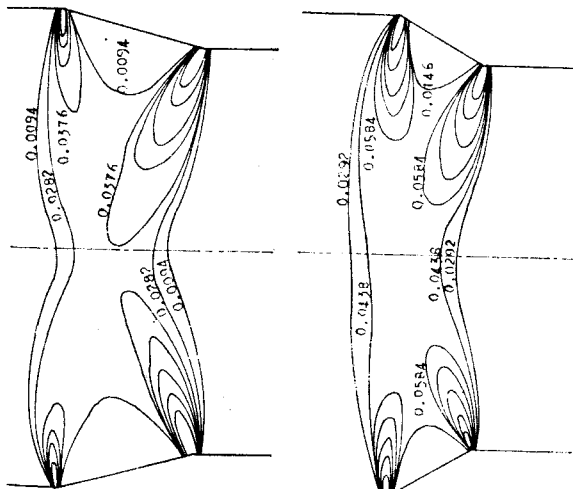
The distributions of equivalent strain rates which result from the distributions of the rotating angles are evaluated as

shown in Figure 5.

When the axis of anisotropy inclines to the direction of extrusion, the texture of the flow metal of specimens appears fibrous, as shown in Figure 6. It has influence on the deformation modes and the strain rates. In the distributions of the equivalent strain rates, it is found that its influence becomes remarkable as the inclination of the anisotropic axis to the direction of extrusion and the semi-angle of die larger, that is, it appears in the distributions of rotating angles, for exa-



(a) Specimen No. 2 (b) Specimen No. 6

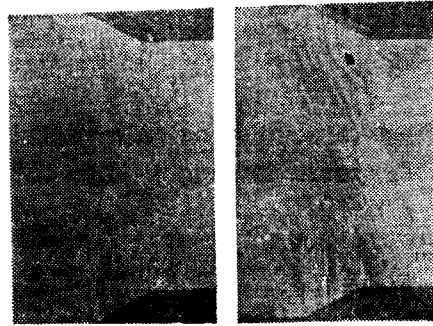


(c) Specimen No. 11 (d) Specimen No. 8

Fig. 5. Distributions of equivalent strain rates

ple, in Figure 5-(d) of the specimen number 8.

And it can be found that with the variation of orientation of specimens to the direction of mechanical treatment, i.e., the axis of anisotropy, the upper portion of the slip line field becomes larger than the lower portion, which is in good agreement with the result obtained from the theory of anisotropy.



(a) Specimen No. 7 (b) Specimen No. 9

Fig. 6. Texture of flow metal

APPENDIX

Slip line field configuration

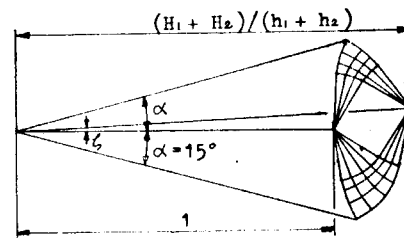
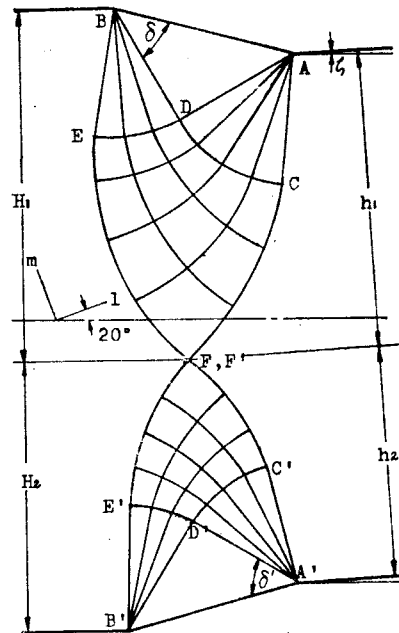


Fig. A-1. Slip line field configuration and hodograph for an extrusion; $\beta=20^\circ$, $\alpha=15^\circ$, $c=0.1$, $r=0.15$

The relationships along the characteristics for an anisotropic material are given by¹⁾

$p/2T+g=\text{constant}$ along an α -line

$p/2T-g=\text{constant}$ along a β -line (A-1)

where

$$g(\phi) = -\frac{\frac{1}{2}c \cdot \sin 2\phi \cdot \cos 2\phi}{(1-c \cdot \sin^2 2\phi)^{\frac{1}{2}}} + \int_0^\phi (1-c \cdot \sin^2 2\phi)^{\frac{1}{2}} d\phi \quad (\text{A-2})$$

Using the above relationship, the slip line field can be constructed as shown in Figure A-1²⁾.

References

1. R. Hill, *Mathematical Theory of Plasticity* Oxford University Press (1950)
2. W. Johnson, M.C. de Malherbe and R. Venter, *Int. J. Mech. Sci.* Vol. 15. pp. 109-116 (1973)
3. R. Venter, W. Johnson and M.C. de Malherbe, *J. Mech. Engng. Sci.* Vol. 13. pp. 416-428 (1971)
4. W. Johnson, M.C. de Malherbe and R. Venter, *J. Mech. Engng. Sci.* Vol. 14. pp. 297-306 (1972)
5. W. Johnson and P.B. Mellor, *Engineering Plasticity*, Van Nostrand Reinhold (1972)
6. W. Prager and P.G. Hodge, *Theory of perfectly Plastic Solids*, John Wiley and Sons (1951)
7. W. Johnson and H. Kudo, *The Mechanics of Metal Extrusion*, Manchester University Press (1962)
8. 金東垣, 大韓機械學會論文集 第一卷, 第一號, pp. 26 大韓機械學會 (1977)
9. 加藤, 室田, 神馬, 日本機械學會誌, 第73卷, 第614號, pp. 371 (1968)
10. 山田, 橫內, 輪竹, 塑性加工春季講演會論文集 pp. 233 日本塑性加工學會 (1972)
11. A.J. Durelli and V.J. Parks, *Moire Analysis of Strain*, Prentice-Hall Inc. (1970)
12. M. Abramowitz and I.A. Stegun, *Handbook of Mathematical Functions*, Dover Publications (1972)